John W. Watts, Jr. and Martin O. Burrell

George C. Marshall Space Flight Center, Huntsville, Alabama

SUMMARY

Sources of high-energy electrons are encountered in space (the magnetically trapped Van Allen belt electrons) and in ground-level high-energy physics laboratories. It is important to be able to predict the damage resulting to human beings and radiation-sensitive equipment near these sources. In this report, various techniques for the calculation of electron and bremsstrahlung dose deposition are described. New energy deposition, transmission, and reflection coefficients for electrons incident on plane slabs for angles of 0, 30, 60, 75, and 89.9 deg and energies of 0.5, 1.0, 2.0, 3.0, 4.0, 5.0, 6.0, and 10.0 MeV are presented, and methods for their use in electron dose calculations are developed. A method for electron dose calculations using the "straight-ahead" approximation is also developed, and the various methods are compared and found to be in good agreement. Accurate and approximate methods of calculating bremsstrahlung dose are derived and compared. The approximation is found to give good order of magnitude estimate of dose where the electron spectrum falls off exponentially with energy. The primary weakness of both calculations is the approximation of the bremsstrahlung source angular distribution; the actual distribution is not easily determined. More work needs to be done in this area.

USE OF BERGER'S MONTE CARLO DATA IN ELECTRON DOSE CALCULATIONS

Probably the most successful attack on the electron transport problem has been by Martin Berger[1-3] using Monte Carlo methods and multiple scattering techniques. His present set of programs will take an incident beam of electrons or photons and follow both the primaries and any secondary electrons or photons produced. The output includes almost any quantity of interest depending on the program option used. Because the simulation is so thorough, the program is very complex and requires large amounts of computer time on one of the larger machines available to complete an accurate calculation. Thus, the program's primary usefulness is in generating basic data for incorporation into other programs using more simplified approaches to the problem.

Berger's program was made available to Marshall Space Flight Center (MSFC), and a number of calculations have been performed here for comparison with experimental work[4]. As a second study systematic calculations covering the energy range of from 0.5 to 10.0 MeV for a number of angles of incidence by a monodirectional beam on a plane aluminum slab were made. The geometry is shown in Fig. 1. Of particular interest were the electron energy and number transmission and reflection and the energy deposition coefficients, because they can be incorporated into an electron dose or number deposition calculation involving an arbitrary incident electron energy and angular distribution. To minimize the computer time used no photons were followed, and only enough electron histories (2500 through 7000, depending on the angle of incidence) were sampled to get good statistics for the reflection, transmission, and deposition coefficients. (A much higher number of histories would have been required to get good statistics on one of the differential quantities such as exiting energy spectrum.) The fact that secondary photons were not followed means that there is a slight underestimate both in the number of coefficients due to missing tertiary electrons produced by the photons and in the energy factors due to energy transported by secondary photons. Because over most of the energy range of interest electrons lose only a small fraction of their energy as photons, both these effects should be small. The radiative yield, the fraction of an

electron's energy lost as bremsstrahlung in stopping, is 0.003324 at 0.25 MeV and 0.07721 at 10.0 MeV in aluminum[2]. This quantity should set an upper bound on the possible error induced by the limitations imposed at least for the energy factors.
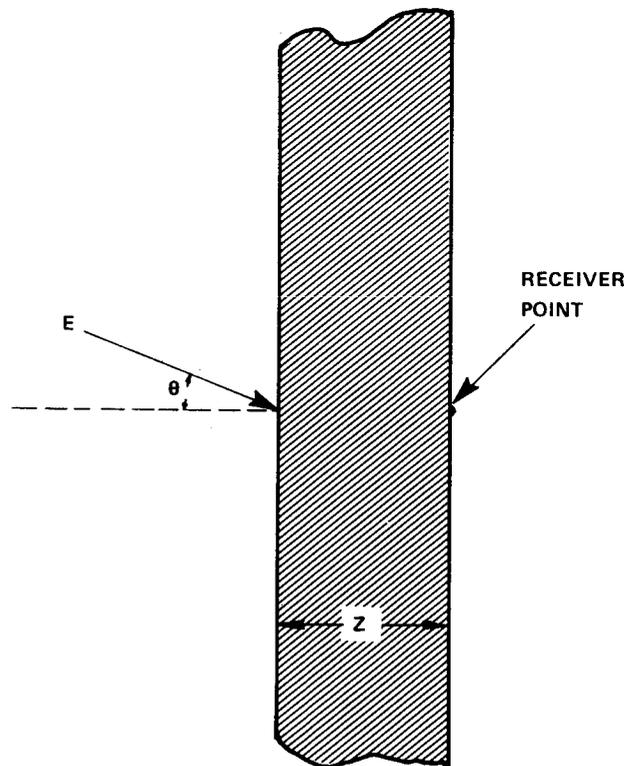

FIGURE 1: BASIC GEOMETRY USED FOR CALCULATIONS

There are several approaches for attacking a dose deposition calculation using the results tabulated by Berger's electron transport program. The most obvious is to use the internal energy spectrum and instantaneous stopping power. Two less obvious but more efficient methods — one reasonably exact and the other approximate — will be described here.

The exact calculation makes use of a quantity Berger calls energy deposition (Figs. 2 and 3), which is the average energy deposited per unit mass per electron at a given depth into a plane, infinitely thick slab by, in this case, a monodirectional beam of electrons. [This does not follow the initial model (Fig. 1) because there is material behind the receiver point.] Berger calculates the energy deposition by breaking up the slab into thin layers and keeping an inventory of energy deposited in each layer and then dividing this quantity by the incident number of initial electron histories and layer thickness. Thus,

$$\rho(E, \theta, X_j) = \frac{\sum_{i=1}^{N_j} \Delta E_{ij}}{N_0 \Delta X_j} \quad , \quad (1)$$

where ρ is the energy deposition in MeV/g/unit current, E is the incident energy in MeV, θ is the incident beam angle measured from the normal to the slab, X_j is the depth to the center of the jth layer, N_j is the number of electrons penetrating layer j, ΔE_{ij} is the energy in MeV deposited by the ith penetrating electron in the jth layer, N_0 is the number of initial electron histories, and ΔX_j is the thickness of the jth layer in g/cm². In Berger's tabulation X_j is measured in fractions of an electron pathlength at the incident energy. The electron mean pathlength is the average length of the zig-zag path followed by an electron in stopping as opposed to the mean range which is the average straight-line distance traversed. It is given by:

$$r_0(E) = \int_E^0 \frac{dE'}{S_T(E')} \quad , \quad (2)$$

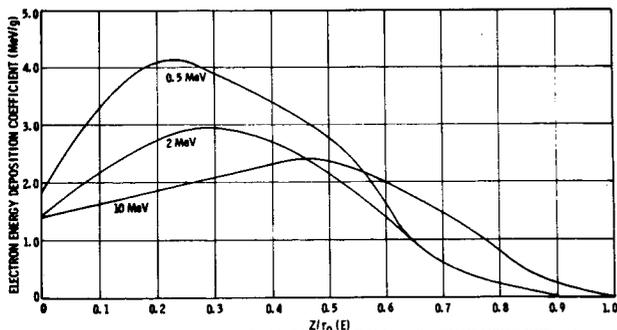where $r_0(E)$ is the pathlength at energy E and $S_t(E')$ is the total instantaneous stopping power.
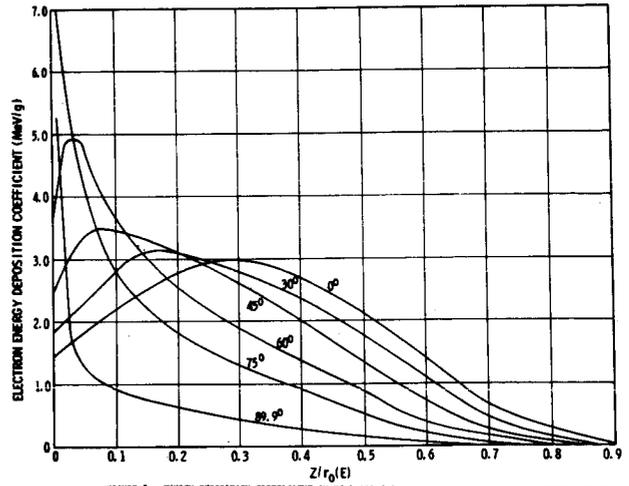

FIGURE 3: ENERGY DEPOSITION COEFFICIENT (MeV/g) FOR 2.0 MeV ELECTRONS INCIDENT AT VARIOUS ANGLES

If there is an angular and energy flux distribution given by $\Phi_0[E, \vec{\Omega}(\theta, \phi)]$ with Φ_0 electrons incident per unit at E and per unit solid angle in the direction $\vec{\Omega}$, then the incident current as used by Berger is

$$J_0(\vec{\Omega}) = \Phi_0(E, \vec{\Omega}) \cos(\theta) \quad , \quad (3)$$

and the dose at a depth Z in g/cm² is given by:

$$D(Z) = K \int_{\vec{\Omega}} \int_E \rho[E, \theta, Z/r_0(E)] \Phi_0(E, \vec{\Omega}) \quad (4)$$

$$\cos \theta \, dE \, d\vec{\Omega} \quad ,$$

where K is a units conversion constant. Dose is more often measured in rads than MeV/g, in which case K = 1.60 x 10⁻⁸ rads/(MeV/g).* In the case where there is a monodirectional beam incident at an angle θ from the slab normal, Equation (4) becomes:

$$D(Z, \theta) = K \cos \theta \int_E \rho[E, \theta, Z/r_0(E)] \quad (5)$$

$$\Phi_0(E) \, dE \quad .$$

Another case of interest is that in which the distribution is half-space isotropic. In this case the dose is given as

$$D_{iso}(Z) = K \int_E \int_0^{\frac{\pi}{2}} \rho[E, \theta, Z/r_0(E)] \quad (6)$$

$$\cos \theta \sin \theta \, d\theta \, \Phi_0(E) \, dE \quad .$$

Thus, a half-space energy deposition function may be defined by

$$\rho_{iso}(E, X) = \int_0^{\frac{\pi}{2}} \rho(E, \theta, X) \quad (7)$$

$$\cos \theta \sin \theta \, d\theta \quad .$$

*To convert rads to SI Units in joules per kilogram, multiply rads by 0.01.

FIGURE 2: ENERGY DEPOSITION COEFFICIENT (MeV/g) AT 0.5, 2.0, AND 10.0 MeV FOR A NORMALLY INCIDENT ELECTRON BEAM

This function is tabulated in Table 1. If Equation (7) is used, Equation (6) becomes:

$$D_{iso}(Z) = K \int_E \rho_{iso} [E, Z/r_0(E)]$$

$$\Phi_0 (E) \, dE \quad . \qquad (8)$$

The approximate method for calculating electron dose makes use of the energy transmission and reflection factor of Berger to derive an approximation to the energy deposition function. The electron energy current transmission and reflection and number current transmission and reflection factor shown in Figs. 4 through 11 are defined as follows:

$$T_N (E, \theta, X) = \frac{N_T (E, \theta, X)}{J_0 (\theta)}$$

$$A_N (E, \theta, X) = \frac{N_R (E, \theta, X)}{J_\phi (\theta)}$$

$$T_E (E, \theta, X) = \frac{\sum_{i=1}^{N_T} E_{Ti} (E, \theta, X)}{E J_0 (\theta)} \qquad (9)$$

$$A_E (E, \theta, X) = \frac{\sum_{i=1}^{N_R} E_{Ri} (E, \theta, X)}{E J_0 (\theta)} \quad ,$$

where T_N is the number transmission factor; N_T is the number of electrons passing through a slab X thick; A_N is the number reflection factor where N_R is the number of electrons reflected from a slab X thick; T_E is the energy transmission factor where E_{Ti} is the energy of the ith transmitted electron; and A_E is the energy reflection factor where E_{Ri} is the energy of the ith reflected electron.
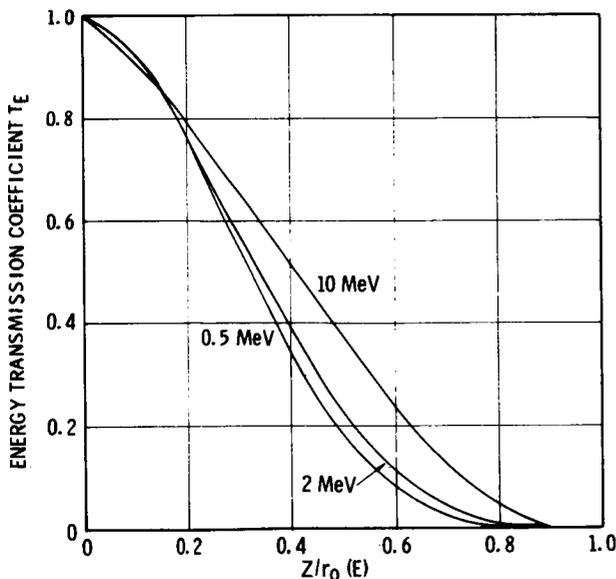
How these factors may be used in energy deposition or dose calculations will now be considered. From conservation of energy,

$$E = E [A_E (E, \theta, X) + U_E (E, \theta, X)$$
$$+ T_E (E, \theta, X)] \qquad (10)$$

or

$$1 = A_E (E, \theta, X) + U_E (E, \theta, X)$$
$$+ T_E (E, \theta, X) \qquad (11)$$

are obtained, where $U_E(E, \Theta, X)$ is the fraction of the energy either deposited in the slab or radiated as bremsstrahlung. Since in the energy range of interest the radiated component is small, it will be assumed negligible. If a quantity $f(X', E, \Theta, X) dX'$ is defined, which is the fraction of the incident energy deposited between X' and X' + dX', then

$$U_E (E, \theta, X) = \int_0^X f (X', E, \theta, X) \, dX' \quad . \qquad (12)$$

Using Equations (11) and (12) yields

$$\int_0^X f(X', E, \theta, X) \, dX' = 1 - A_E (E, \theta, X)$$
$$- T_E (E, \theta, X) \quad . \qquad (13)$$

Taking the derivative with respect to X gives

$$f(X, E, \theta, X) + \int_0^X \frac{df}{dX} (X', E, \theta, X) \, dX' =$$
$$- \frac{d}{dX} [A_E (E, \theta, X) + T_E (E, \theta, X] \quad . \qquad (14)$$

FIGURE 4: ENERGY TRANSMISSION COEFFICIENT AT 0.5, 2.0, AND 10.0 MeV FOR A NORMALLY INCIDENT ELECTRON BEAM
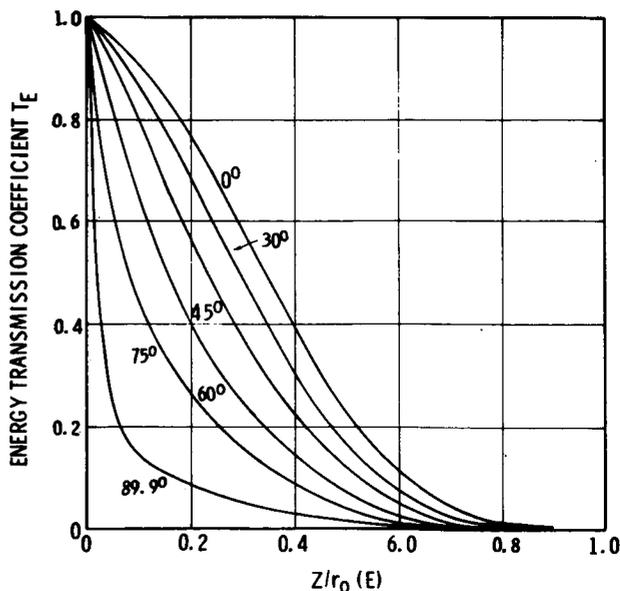

FIGURE 5: ENERGY TRANSMISSION COEFFICIENT FOR 2.0 MeV ELECTRONS INCIDENT AT VARIOUS ANGLES
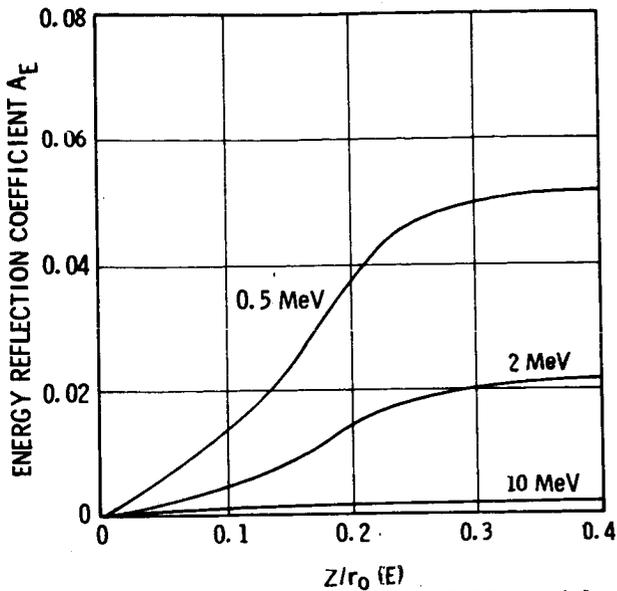
FIGURE 6: ENERGY REFLECTION COEFFICIENT AT 0.5, 2.0, AND 10.0 MeV FOR A NORMALLY INCIDENT ELECTRON BEAM
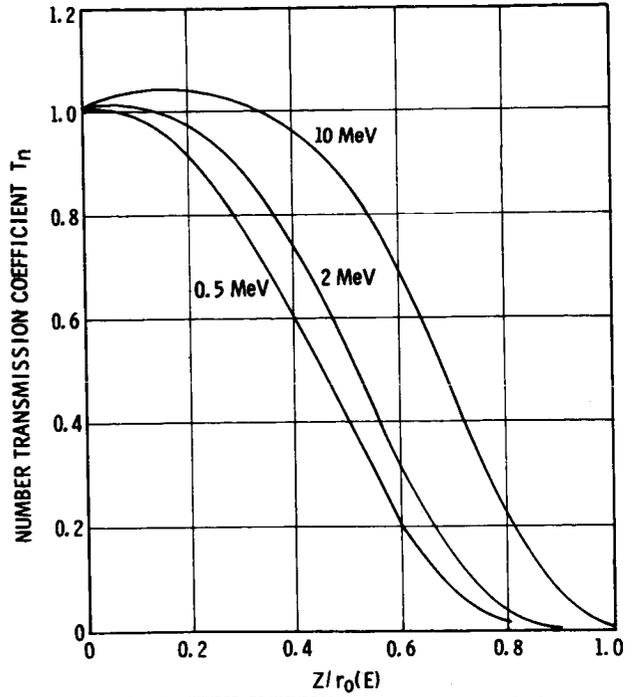

FIGURE 8: NUMBER TRANSMISSION COEFFICIENT AT 0.5, 2.0, AND 10.0 MeV FOR A NORMALLY INCIDENT ELECTRON BEAM
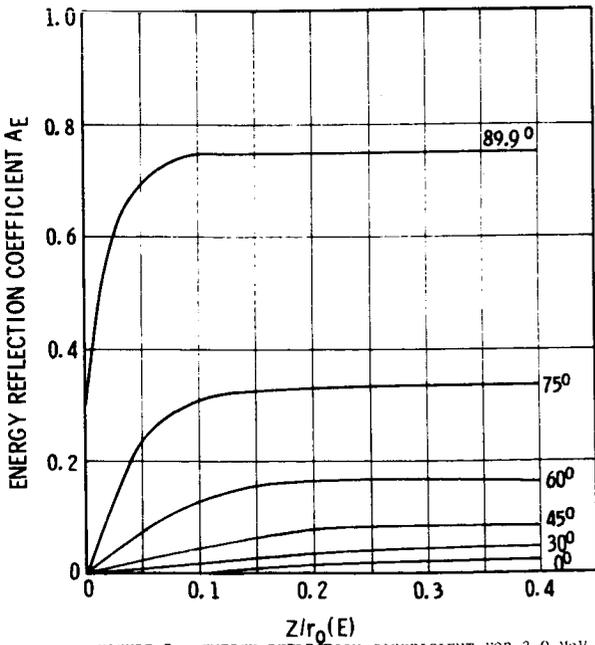

FIGURE 7: ENERGY REFLECTION COEFFICIENT FOR 2.0 MeV ELECTRONS INCIDENT AT VARIOUS ANGLES
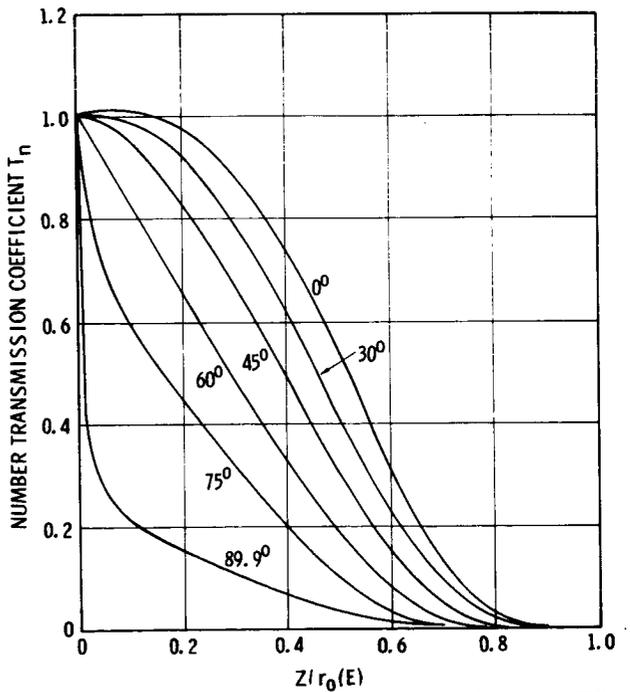

FIGURE 9: NUMBER TRANSMISSION COEFFICIENT FOR 2.0 MeV ELECTRONS INCIDENT AT VARIOUS ANGLES
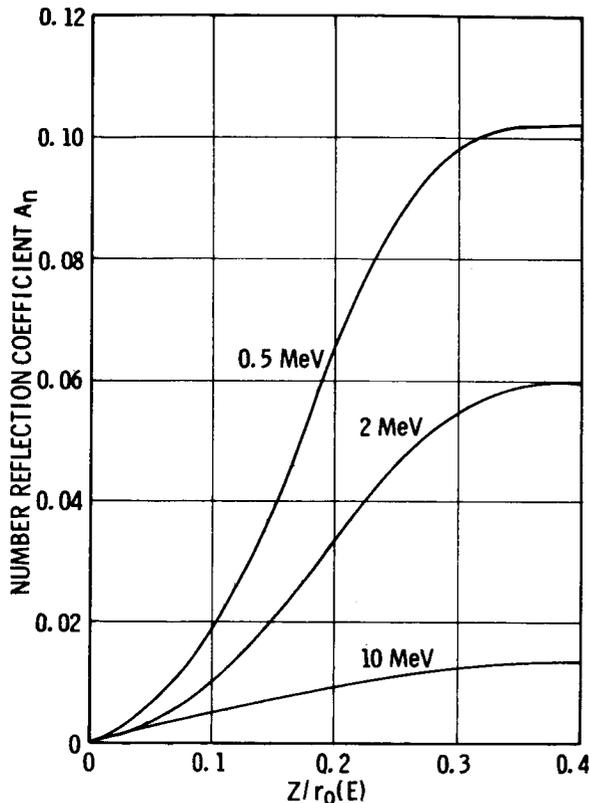
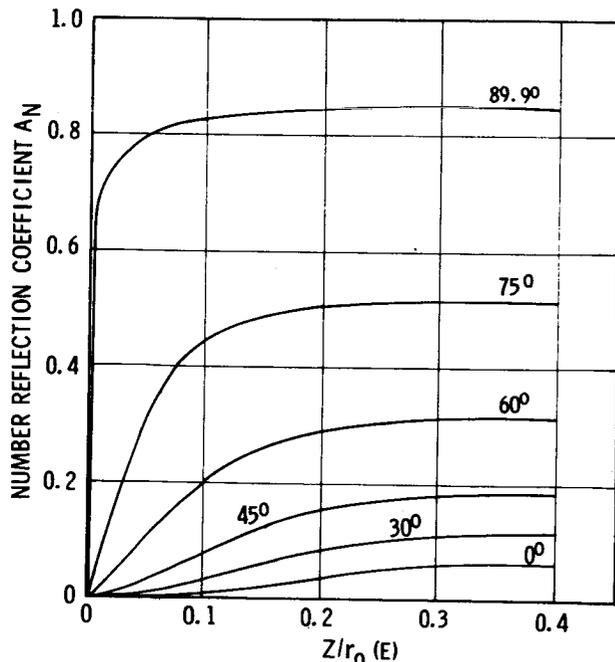FIGURE 10: NUMBER REFLECTION COEFFICIENT AT 0.5, 2.0, AND 10.0 MeV FOR A NORMALLY INCIDENT ELECTRON BEAM

FIGURE 11: NUMBER REFLECTION COEFFICIENT FOR 2.0 MeV ELECTRONS INCIDENT AT VARIOUS ANGLES

The approximation in this method involves ignoring the integral term on the left in this equation. Since $f(X',E,\Theta,X)$ increases with increasing X (due to reflected electrons), the derivative is always greater than or equal to zero. Thus the integral is positive, and ignoring it gives a conservative estimate of $f(X,E,\Theta,X)$. It is difficult to justify this approximation except to observe that in practice it yields results comparable with those of the previously described method. It was developed because Berger's older publication presented only the transmission and reflection factors, the energy deposition factor having become available only recently.

The energy deposition function (in units of MeV/g) is given by:

$$\rho(X,E,\theta,X) = \frac{Ef(X,E,\theta,X)}{r_0(E)} \qquad (15)$$

or

$$\rho(X,E,\theta,X) \approx \frac{-E\,d}{r_0(E)\,dX}\,[A_E(E,\theta,X) + T_E(E,\theta,X)] \qquad (16)$$

It is interesting to note that $f(X',E,\Theta,X)$ for $X' < X$ always has a contribution caused by reflection from portions of the shield beyond X' but that $f(X,E,\Theta,X)$ does not. Thus it approximates the quantity needed for an energy deposition calculation in our original geometry.

Because of the definition of ρ in the derivations the material of the receiver must be the same as that of the shield. An approximate correction for estimating the dose for a different receiver can be made by multiplying the single material calculation by the ratio of the collision stopping power in the shield material at some typical energy for the exiting electron spectrum. Fortunately, the energy selected is not particularly important since the ratio of two electron stopping powers is not a sensitive function of energy except at very low energies (> 0.01 MeV). Some estimate of the accuracy of the approximation can be found by observing the variation of the ratio with energy. A particularly interesting case is that of an aluminum shield and a tissue receiver. This case, using Berger's stopping power data[3] is given in Table 2.

Taking the simple average of ratios between energies of 0.1 to 10.0 MeV yields a correction (1.30) that will be within about 3% of an exact calculation under most conceivable conditions. (For typical incident energy spectra encountered, it would be unusual for the average energy of the exiting spectrum to be less than 0.04 MeV). Thus, for an aluminum shield and a tissue receiver Equations (5) and (6) become, respectively:

$$D(Z,\theta) = 1.3\,K\cos\theta \int_E \rho[E,\theta,Z/r_0(E)]\,\Phi_0(E)\,dE \qquad (17)$$

and

$$D_{iso}(Z) = 1.3\,K \int_E \rho_{iso}[E,Z/r_0(E)]\,\Phi_0(E)\,dE \qquad (18)$$

805

TABLE 1: ELECTRON FLUX ENERGY DEPOSITION COEFFICIENTS (MeV/g) FOR A HALF-SPACE ISOTROPIC INCIDENT BEAM ON AN ALUMINUM SEMI-INFINITE PLANE SHIELD

INCIDENT ENERGY (MeV) SHIELD THICKNESS (PATHLENGTHS)	.9	1	2	3	4	5	6	7
0.01	1.8151	1.8365	1.7236	1.6841	1.6654	1.6367	1.6544	1.6312
0.03	2.1534	1.8364	1.6960	1.6611	1.6449	1.6532	1.6632	1.6672
0.05	2.1410	1.8097	1.6726	1.6446	1.6290	1.6103	1.6240	1.6333
0.07	2.1133	1.7640	1.6382	1.5869	1.5760	1.5748	1.5872	1.5559
0.09	2.0430	1.7235	1.5597	1.5869	1.5399	1.5243	1.5133	1.4976
0.11	2.0211	1.6735	1.5509	1.5095	1.4711	1.4695	1.4764	1.4962
0.13	1.9486	1.6359	1.4837	1.4652	1.4534	1.4222	1.4441	1.4839
0.15	1.9542	1.6299	1.4860	1.4269	1.4095	1.4239	1.4048	1.3889
0.17	1.8698	1.6371	1.4481	1.3941	1.3847	1.4010	1.3827	1.3841
0.19	1.8955	1.5668	1.3903	1.3376	1.3439	1.3503	1.3462	1.3306
0.21	1.8020	1.4981	1.3642	1.3056	1.2928	1.2745	1.2738	1.2847
0.23	1.7683	1.4329	1.3028	1.2633	1.2581	1.2417	1.2346	1.2476
0.25	1.7289	1.3648	1.2463	1.2305	1.2192	1.2259	1.2228	1.2061
0.27	1.6721	1.3380	1.2159	1.1777	1.1836	1.1872	1.1895	1.1788
0.29	1.5832	1.2992	1.1811	1.1602	1.1420	1.1408	1.1312	1.1466
0.31	1.5492	1.2267	1.1246	1.0882	1.0969	1.1041	1.0742	1.1131
0.33	1.4704	1.1598	1.0788	1.0836	1.0733	1.0640	1.0393	1.0729
0.35	1.4457	1.1320	1.0844	1.0351	1.0293	1.0376	1.0530	1.0419
0.37	1.3611	1.0937	1.0417	0.9843	0.9980	1.0230	1.0055	0.9807
0.39	1.3184	1.0611	0.9815	0.9547	0.9441	0.9551	0.9695	0.9377
0.41	1.2098	1.0084	0.9216	0.8826	0.8778	0.8997	0.8995	0.8993
0.43	1.0848	0.9315	0.8696	0.8378	0.8133	0.8341	0.8810	0.8775
0.45	1.0022	0.8712	0.8082	0.7828	0.7864	0.8159	0.8054	0.8375
0.47	0.9440	0.7738	0.7613	0.7465	0.7295	0.7477	0.7539	0.7936
0.49	0.8853	0.7233	0.7133	0.6884	0.7006	0.7036	0.7048	0.7463
0.51	0.8172	0.6981	0.6661	0.6307	0.6677	0.6679	0.6594	0.7232
0.53	0.6549	0.6745	0.6156	0.6941	0.5936	0.6039	0.6301	0.6680
0.55	0.6457	0.5897	0.5624	0.5413	0.5393	0.5531	0.5762	0.6225
0.57	0.5520	0.4653	0.4842	0.4622	0.4384	0.5051	0.5445	0.5799
0.59	0.4438	0.3992	0.4042	0.4224	0.4393	0.4635	0.4996	0.5380
0.61	0.3956	0.3124	0.3259	0.3636	0.3962	0.4245	0.4466	0.4999
0.63	0.3164	0.2719	0.2944	0.3108	0.3449	0.3597	0.3759	0.4677
0.65	0.2498	0.2428	0.2522	0.2786	0.3101	0.3019	0.3479	0.4242
0.67	0.2034	0.1848	0.2151	0.2323	0.2666	0.2647	0.3081	0.3790
0.69	0.1744	0.1590	0.1889	0.1921	0.2251	0.2256	0.2643	0.3315
0.71	0.1310	0.1248	0.1395	0.1655	0.1776	0.1981	0.2292	0.2943
0.73	0.1031	0.0565	0.1083	0.1340	0.1513	0.1628	0.1937	0.2624
0.75	0.0812	0.0740	0.0893	0.1014	0.1254	0.1394	0.1572	0.2139
0.77	0.0519	0.0548	0.0722	0.0778	0.0947	0.1110	0.1320	0.1822
0.79	0.0417	0.0355	0.0518	0.0592	0.0730	0.0859	0.1078	0.1603
0.81	0.0274	0.0271	0.0329	0.0429	0.0581	0.0651	0.0800	0.1236
0.83	0.0098	0.0162	0.0219	0.0295	0.0429	0.0503	0.0555	0.1045
0.85	0.0069	0.0119	0.0115	0.0192	0.0307	0.0316	0.0424	0.0770
0.87	0.0036	0.0060	0.0077	0.0169	0.0199	0.0253	0.0283	0.0578
0.89	0.0031	0.0023	0.0064	0.0050	0.0225	0.0170	0.0172	0.0475
0.91	0.0026	0.0004	0.0018	0.0036	0.0053	0.0107	0.0145	0.0368
0.93	0.0012	0.0004	0.0018	0.0018	0.0060	0.0050	0.0110	0.0221
0.95	0.0000	0.0004	0.0000	0.0025	0.0028	0.0050	0.0072	0.0131
0.97	0.0000	0.0000	0.0000	0.0000	0.0004	0.0014	0.0041	0.0102
0.99	0.0000	0.0000	0.0000	0.0000	0.0004	0.0000	0.0009	0.0060

Energy (MeV)	$R = \dfrac{dE/dX \text{ tissue}}{dE/dX \text{ aluminum}}$	$\dfrac{R-1.3}{R} \times 100$ (%)
0.01	1.383	6.0
0.02	1.350	3.7
0.04	1.325	1.9
0.06	1.313	1.0
0.08	1.305	0.4
0.1	1.300	0.0
0.2	1.285	-1.2
0.4	1.276	-1.9
0.6	1.272	-2.2
0.8	1.271	-2.3
1.0	1.272	-2.2
2.0	1.281	-1.5
4.0	1.301	0.1
6.0	1.317	1.3
8.0	1.329	2.2
10.0	1.340	3.0

Curve fits of $\rho(E,\Theta,X)$ have been found to be very useful for computational purposes. Fit over X of the form

$$\rho(E,\theta,X) = e^{\sum\limits_{i=1}^{N} A_i X^{i-1}} \qquad (19)$$

has been found to give satisfactory results for normal incidence and half-space isotropic incidence, two cases of special interest. Fits of the above form were made and then the coefficients were fit as a function of energy. For normal incidence the coefficients are given by:

$$A_1 = 0.913\, e^{0.963E} + 0.021E + 0.215$$
$$A_2 = 5.0 - 0.491E$$
$$A_3 = 57.573\,(E - 5.0)/(E + 29.98) \qquad (20)$$
$$A_4 = -1.6E^{0.837} \quad ,$$

and for half-space isotropic the coefficients are given by:

$$A_1 = 0.52 + 0.09854\, E^{-1.468}$$
$$A_2 = e^{-0.821E} - 1.0$$
$$A_3 = -2.5 \left(e^{-1.022E} + 1.0 \right) \qquad (21)$$
$$A_4 = 3.253\, e^{-0.323E} + 5.8$$
$$A_5 = -15.4375 + 1.5542E - 0.0786077E^2 \quad .$$

Because the shape of the energy deposition function for angles near 90 deg is different from that near 0 deg, a good fit by a single functional form is difficult to achieve over the whole range of directions. Best results will probably be obtained by interpolation from the actual data or a smoothed set derived from it. The function $f(E,\Theta, X)$ derived using the reflection and transmission factors was also fit but by a different form. The fit was to the form

$$1 - T_E(E,\theta,X) - A_E(E,\theta,X) = \qquad (22)$$

$$A\left[1 - e^{(BX + CX^2 + DX^3)} \right] \quad ,$$

where A, B, C, and D are functions of E and Θ.
Then, taking the derivative with respect to X and using Equation (14) yields

$$f(E,\theta,X) = \tag{23}$$

$$-A(B + 2CX + 3DX^2) e^{(BX + CX^2 + DX^3)}$$

Fits have been derived for the two cases of special interest. For a normally incident beam ($\Theta = 0$ deg) in the energy range 0.5 to 10.0 MeV,

$$A = \frac{0.893 + 1.682E}{1.0 + 1.665E}$$

$$B = \frac{11.0E}{11.0E + 6.0} \tag{24}$$

$$C = 4.2 \exp(-0.47E)$$

and

$$D = 5.16 \quad.$$

Berger has published a transmission and reflection coefficient for a cosine law source (half-space isotropic flux)[3]. In this case f_{iso} (E,X) is a relatively insensitive function of E, and satisfactory results are obtained by taking an average curve for all energies. For energy deposition,

$$A = 0.439$$
$$B = -2.08$$
$$C = -3.54 \tag{25}$$
$$D = -6.08$$

The electron pathlength $r_0(E)$ in aluminum taken from Berger[2] has also been fit by the following form:

$$r_0(E) = \tag{26}$$

$$(1.33 - 0.019E)\left(\sqrt{0.2713E^2 + 0.0121} - 0.11\right),$$

which is within 2% of actual curves for energies greater than 0.3 MeV and within 5% between 0.2 and 0.3 MeV.

ELECTRON TRANSPORT USING THE STRAIGHT-AHEAD AND CONTINUOUS SLOWING DOWN APPROXIMATIONS

A method commonly used for describing the transport of protons is to assume that the particle travels through the shield along its incident direction losing energy continuously according to some stopping power law. Thus, according to the approximations, the energy and direction of the particle at any point in the shield is completely predictable. This method has the advantage of providing an energy spectrum at the internal point of interest that may be used to determine such things as secondary production sources as well as to calculate dose deposition. Its disadvantages for application to electron transport are twofold: First, electrons are more likely to be scattered from their original direction than protons, and

*This mean range is not Berger's mean pathlength.

second, electrons can suffer large energy losses in a single interaction. Thus the straight-ahead approximations should not be expected to be especially applicable. The approximations have been applied with some success, however.

Since the validity of the approximations in applications to electron transport are somewhat questionable, one would prefer to be on the conservative side in any estimate of particle energy or number. By using the extrapolated electron range rather than the mean range* for definition of other required quantities this can be accomplished. The extrapolated range is defined as shown in Fig. 12, where it can be seen that few electrons penetrate beyond this distance. A very good fit to the extrapolated range in aluminum is given by:

$$r_{ex} = R(E) = \sqrt{\frac{E^2}{a} + b^2} - b \tag{27}$$

over the energy range from 0.0 to 16.0 MeV. For R(E) in g/cm^2, E is in MeV, a is 1.92, and b is 0.11[5].
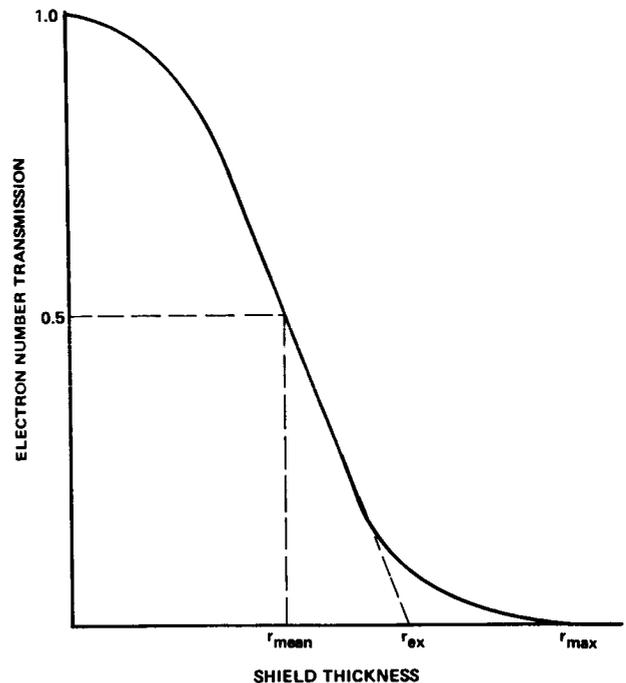

FIGURE 12: DEFINITIONS OF ELECTRON MEAN RANGE r_{MEAN}, EXTRAPOLATED RANGE r_{ex}, AND MAXIMUM RANGE r_{max}

Given the electron range, one can determine the relationship between the initial energy and the energy after passing through thickness Z of material as follows:

Since

$$R(E) = R(E') + Z \quad, \tag{28}$$

where E is the initial energy and E' is the energy at depth Z,

808

$$E = g(E', Z) = R^{-1}[R(E') + Z];$$ (29)

R^{-1} denotes the inverse of the function R. Thus, using Equations (27) and (29) gives

$$E = g(E', Z) = \cfrac{1}{a\sqrt{\left[\sqrt{\left(\dfrac{E'}{a}\right)^2 + b^2} + z\right]^2 - b^2}}$$ (30)

The relationship between the external differential flux $\Phi_0(E)$ and the flux at depth Z, $\Phi_Z(E')$, is given by:

$$\Phi_Z(E') = \Phi_0[g(E', Z)]\frac{dg(E', Z)}{dE'}$$ (31)

The derivative enters the equation because of change of energy E to E' units; or as one can see, lower energy electrons lose energy faster, thus changing particle densities. Using Equation (30) gives

$$\frac{dg(E', Z)}{dE'} = \cfrac{E'\left[\sqrt{\left(\dfrac{E'}{a}\right)^2 + b^2} + z\right]}{a\sqrt{\left(\dfrac{E'}{a}\right)^2 + b^2}\sqrt{\left[\sqrt{\left(\dfrac{E'}{a}\right)^2 + b^2} + z\right]^2 - b^2}}$$ (32)

The electron dose deposited at depth Z is given by:

$$D(Z) = K\int_E \Phi_Z(E') S(E') dE'$$ (33)

where S(E') is the instantaneous collision stopping power in the receiver. One can derive an approximation for the stopping power by using the derivative of the range

$$S(E') = -\frac{1}{\dfrac{dR(E')}{dE'}}$$ (34)

$$S(E') = \frac{a^2}{E'}\sqrt{\left(\frac{E'}{a}\right)^2 + b^2}$$ (35)

By a fortunate accident the approximate stopping power derived from aluminum extrapolated range data is a good fit to tissue collision stopping power. (Tissue is the receiver most commonly used.) The fit is within 5% of Berger's tabulated data[2] in the interval 0.15 to 4.5 MeV and within 13% from 0.08 to 10.0 MeV.

Combining the results of Equations (31), (32), (33), and (35) and simplifying the tissue dose behind an aluminum shield Z thick yields
$$D(Z) =$$

$$K\int_{E'} \Phi_0\left[g(E', Z)\right]\cfrac{a\left[\sqrt{\left(\dfrac{E'}{a}\right)^2 + b^2} + Z\right]}{g(E', Z)} dE'.$$ (36)

Equation (36) is derived for normal incidence. For a beam incident at angle Θ to the normal, Z is replaced in the equation by the slant distance to the dose point, Z/cos Θ, and for half-space isotropic flux the dose is given by:

$$D_{iso}(Z) = K\int_0^{\frac{\pi}{2}} \int_{E'} \Phi_0[g(E', Z/\cos\theta)]\cfrac{a\left[\sqrt{\left(\dfrac{E'}{a}\right)^2 + b^2} + Z/\cos\theta\right]}{g(E', Z/\cos\theta)} dE' \sin\theta\, d\theta$$ (37)

COMPARISON OF THE THREE METHODS FOR DOSE CALCULATION

Typical electron spectra encountered in practical applications are exponential in nature. Figures 13 through 18 show comparisons of the three methods for spectra of the form

$$\Phi_0(E) = Pe^{-PE}$$ (38)

where P varies from 0.25 to 6.0. The energy integration limits are 0.0 to 20.0 MeV. The agreement among the three methods is fairly good considering the magnitude of the attenuation that occurs. The two methods using Berger's data have significant disagreement only for high shield thicknesses and isotropic spectra. The disagreement here is probably because a significant fraction of the dose is from electrons with energies above 10 MeV where both methods are using extrapolation on the data. The disagreement between the methods using Berger's data and the straight-ahead method are somewhat larger, but the errors still are not so large as to cause question about the validity of any one of the three approaches.
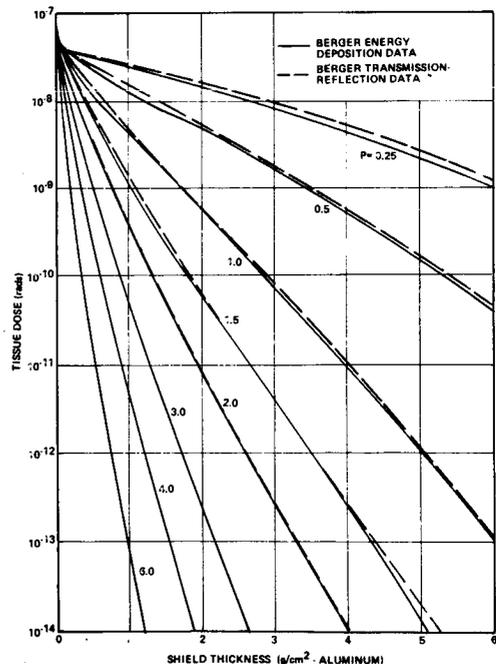

FIGURE 13: COMPARISON OF ELECTRON TISSUE DOSES CALCULATED USING BERGER'S ENERGY DEPOSITION DATA AND TRANSMISSION – REFLECTION DATA FOR A NORMALLY INCIDENT SPECTRUM OF THE FORM $\Phi_0(E) = P \exp(-PE)e/cm^2 - MeV$
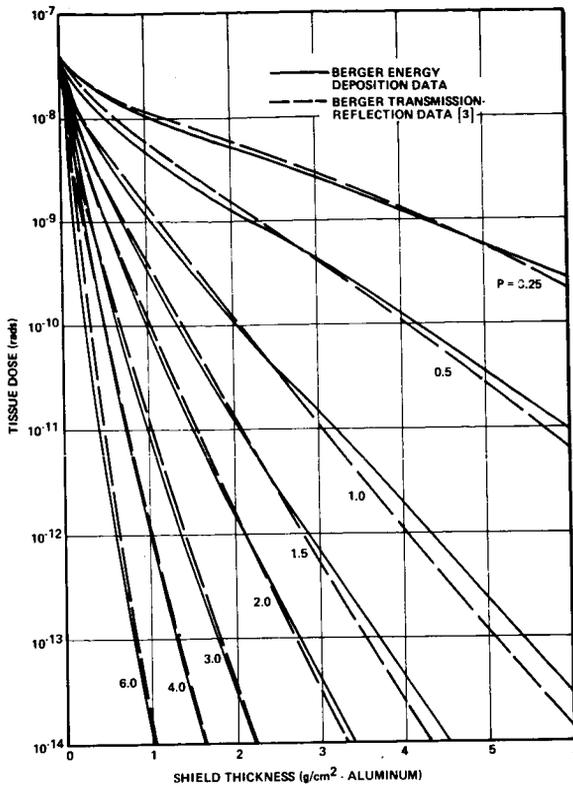
FIGURE 14: COMPARISON OF ELECTRON TISSUE DOSES CALCULATED
USING BERGER'S ENERGY DEPOSITION DATA AND
TRANSMISSION - REFLECTION DATA FOR A HALF-SPACE
ISOTROPIC INCIDENT SPECTRUM OF THE FORM $\phi_o(E) =$
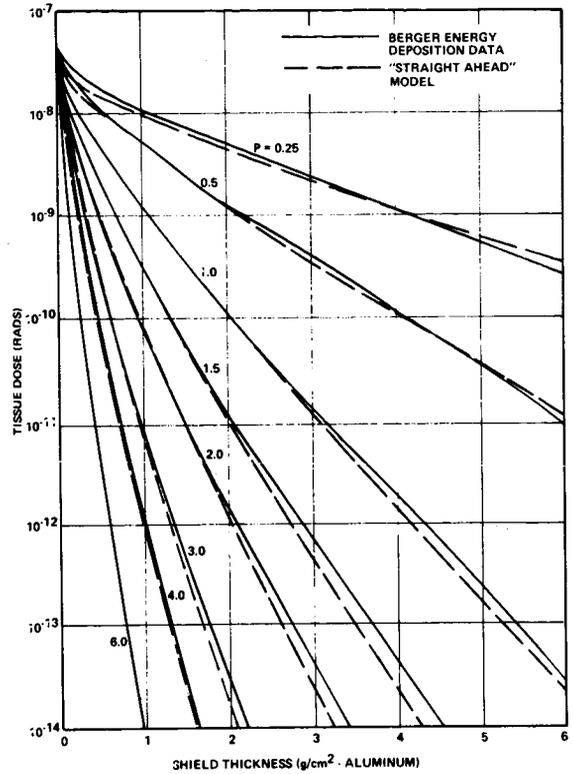$P \exp(-PE)e/cm^2 - MeV$

FIGURE 16: COMPARISON OF ELECTRON TISSUE DOSES CALCULATED
USING BERGER'S ENERGY DEPOSITION DATA AND THE
STRAIGHT-AHEAD MODEL FOR A HALF-SPACE ISOTROPIC
INCIDENT ELECTRON SPECTRUM OF THE FORM $\phi_o(E) =$
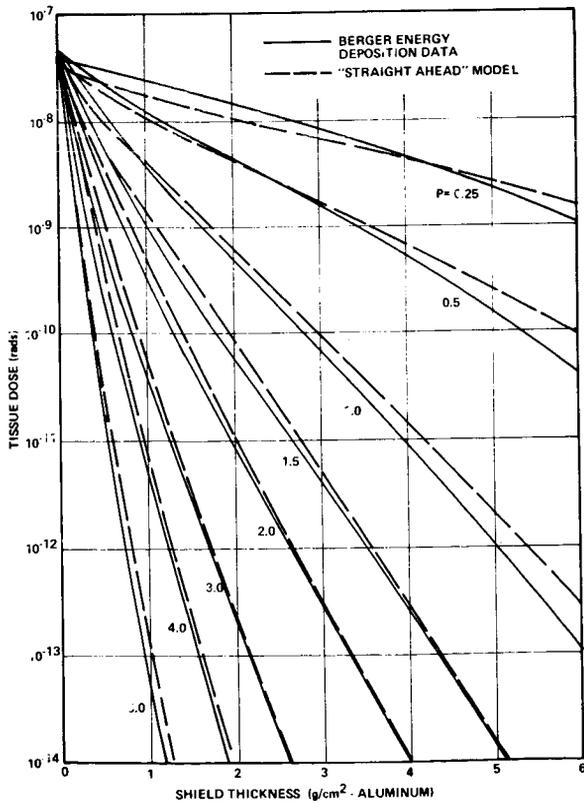$P \exp(-PE)e/cm^2 - MeV$

FIGURE 15: COMPARISON OF ELECTRON TISSUE DOSES CALCULATED
USING BERGER'S ENERGY DEPOSITION DATA AND THE
STRAIGHT-AHEAD MODEL FOR A NORMALLY INCIDENT
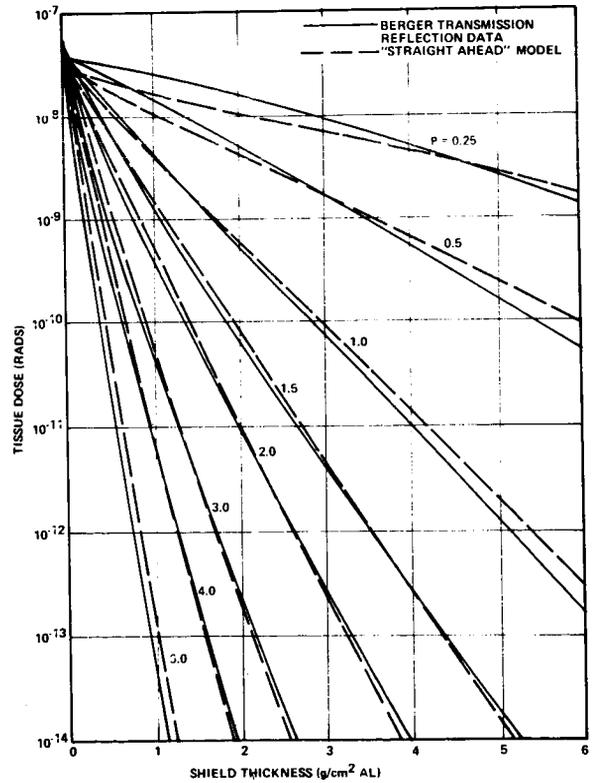SPECTRUM OF THE FORM $\phi_o(E) = P \exp(-PE)e/cm^2 - MeV$

FIGURE 17: COMPARISON OF ELECTRON TISSUE DOSES CALCULATED
USING BERGER'S TRANSMISSION-REFLECTION DATA AND
THE STRAIGHT-AHEAD MODEL FOR A NORMALLY INCIDENT
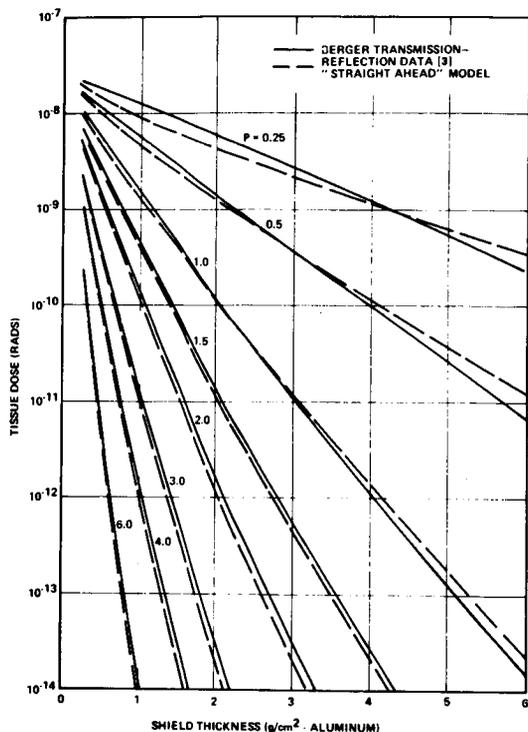SPECTRUM OF THE FORM $\phi_o(E) = P \exp(-PE)e/cm^2 - MeV$

810

FIGURE 18: COMPARISON OF ELECTRON TISSUE DOSES CALCULATED USING BERGER'S TRANSMISSION-REFLECTION DATA AND THE STRAIGHT-AHEAD MODEL FOR A HALF-SPACE ISOTROPIC INCIDENT SPECTRUM OF THE FORM $\zeta_0(E) = P \exp(-PE)$ e/cm² - MeV

BREMSSTRAHLUNG DOSE CALCULATIONS

Previously, consideration has been confined to the dose deposited by electrons; this is satisfactory for thin shields. However, when the shields are thick enough to remove a large fraction of the primary electrons, dose deposition by bremsstrahlung must be taken into account. (The point where this occurs is usually less than 3.0 g/cm².) To do a bremsstrahlung dose calculation one must generate a bremsstrahlung source distribution and then transport the bremsstrahlung from this source to the dose point. To generate the bremsstrahlung source distribution, one needs the electron energy and angular distribution at the source point and the bremsstrahlung production cross section.

Because the interior electron angular distribution is not easily determined and since the bremsstrahlung production cross section differentials in angle are not particularly accurate, a simplification commonly made is to use cross section differential in photon energy only and to make some assumption about the bremsstrahlung source angular distribution. (This assumption will be examined later.) In this case, the bremsstrahlung differential energy flux source or depth Z' and photon energy E_γ is given by:

$$S(E_\gamma, Z') =$$
$$\int_E \int_{\vec{\Omega}} E_\gamma \sum(E_\gamma, E) \, \Phi_{Z'}(E, \vec{\Omega}) \, dE d\vec{\Omega} \qquad (39)$$

in units of MeV/(MeV-g), where $\Sigma(E_\gamma, E)$ is the macroscopic bremsstrahlung production cross

section differential in photon energy in units of photons/g-MeV-(e/cm²) and $\Phi_{Z'}(E, \vec{\Omega})$ is the electron energy and angular distribution at depth Z in units of e/cm²-MeV-sr.

The macroscopic cross section is given by:

$$\sum(E_\gamma, E) = \frac{N_0}{A} \frac{d\sigma}{dE_\gamma} \qquad , \qquad (40)$$

where N_0 is Avagadro's number 6.02×10^{23} atom/mole, A is the atomic weight of the material at the source point in g/mole, and $d\sigma/dE$ is the microscopic bremsstrahlung production cross section differential in photon energy in units of photons/atom . (e/cm²) . MeV. The microscopic cross section presently used for the MSFC calculation is given by:

$$\frac{d\sigma}{dE_\gamma} = F_E(E, E_\gamma) C(E) \frac{Z_0^2 r_0^2 P}{137 E_\gamma P_0}$$

$$\left(\frac{4}{3} - 2 H_0 H \left(\frac{P^2 + P_0^2}{P^2 P_0^2} \right) + \frac{\epsilon_0 H}{P_0^3} + \frac{\epsilon H_0}{P^3} \right.$$

$$- \frac{\epsilon \epsilon_0}{P_0 P} + L \left\{ \frac{8 H_0 H}{3 P_0 P} + \frac{K^2 (H_0^2 H^2 + P_0^2 P^2)}{P_0^3 P^3} \right.$$

$$+ \frac{K}{2 P_0 P} \left[\left(\frac{H_0 H + P_0^2}{P_0^3} \right) \epsilon_0 \right.$$

$$- \left(\frac{H_0 H + P^2}{P_3} \right) \epsilon$$

$$\left. \left. + \frac{2 K H_0 H}{P^2 P_0} \right] \right\} \right) \quad , \qquad (41)$$

where

$$L = 2 \ln \left(\frac{H_0 H + P_0 P - 1}{K} \right)$$
$$\epsilon_0 = \ln \left(\frac{H_0 + P_0}{H_0 - P_0} \right)$$
$$\epsilon = \ln \left(\frac{H + P}{H - P} \right) \quad .$$

The terms H_0 and H are the initial and final total electron energies in mc² units given by

$$H_0 = \frac{E}{mc^2} + 1$$

$$H = \frac{E - E_\gamma}{mc^2} + 1 \quad ;$$

P_0 and P are the initial and final electron momenta given by

$$P_0 = \sqrt{H_0^2 - 1}$$

$$P = \sqrt{H^2 - 1} \quad ;$$

and K is the photon energy or momentum in mc² or mc units, respectively,

$$K = \frac{E_\gamma}{mc^2} \quad .$$

811

The term Z_0 is the atomic number of the source material, r_0 is the classical electron radius 2.82×10^{-13} cm, mc^2 is the rest mass energy of an electron, and $F_E(E,E_\gamma)$ and $C(E)$ are two correction factors. Except for the correction factors this is formula 3BN from Koch and Motz[6], who give a complete description of the cross section. The correction factor $F_E(E,E_\gamma)$ given by

$$
F_E(E,E_\gamma) =
\begin{cases}
\dfrac{\beta_0 \left(1 - e^{\frac{2\pi Z_0}{137 \beta_0}}\right)}{\beta \left(1 - e^{\frac{2\pi Z_0}{137 \beta}}\right)} & \text{for }
\begin{array}{l} E < 2.0 \text{ MeV} \\ \dfrac{E}{E_\gamma} > 0.01 \end{array} \quad (42) \\[1em]
1.0 & \text{otherwise} \quad ,
\end{cases}
$$

where

$$
\beta_0 = \sqrt{1 - \left(\frac{mc^2}{E + mc^2}\right)^2} \qquad (43)
$$

and

$$
\beta = \sqrt{1 - \left(\frac{mc^2}{E - E_\gamma + mc^2}\right)^2} \quad , \qquad (44)
$$

is the Elwert nonrelativistic coulomb correction, and the correction $C(E)$ is an empirical screening correction as shown by Koch and Motz[6]. Koch and Motz further discuss both these corrections[6].

The prime advantage of the straight-ahead approximation is that it does provide an electron spectrum at a given depth. Thus, using the result derived, for a normally incident electron beam, the bremsstrahlung source is given as

$$
S_N(E_\gamma, Z') =
$$
$$
\int_E E_\gamma \sum(E_\gamma, E) \Phi_0 [g(E,Z')] \frac{dg(E,Z')}{dE} dE \quad , \qquad (45)
$$

and for a half-space isotropic incident electron distribution the bremsstrahlung source is

$$
S_{iso}(E_\gamma, Z') = \int_0^{\frac{\pi}{2}} \int_E E_\gamma \sum(E_\gamma, E)
$$
$$
\Phi_0 [g(E, Z'/\cos\theta)] \frac{dg(E, Z'/\cos\theta)}{dE} dE \sin\theta \, d\theta \quad , \qquad (46)
$$

where Φ_0, g, and dg/dE are as defined in the third section.

The bremsstrahlung transport and dose calculation is relatively straightforward for a plane slab geometry given the source energy distribution and some source angular distribution. Using point kernel attenuation with dose build-up factors, the dose is given by:

$$
D(Z) = K \int_{E_\gamma} \int_0^Z \mu_E(E_\gamma) S(E,Z') B(E_\gamma, Z, Z')
$$
$$
G[\mu_m(E_\gamma)|Z-Z'|] \, dE_\gamma \, dZ' \quad , \qquad (47)
$$

where $\mu_E(E_\gamma)$ is the gamma ray energy absorption coefficient [7] for the receiver material; Z is the shield thickness; $B(E,Z,Z')$ is a dose buildup factor, depending on the source angular distribution chosen; and $G[\mu_m(E_\gamma)|Z-Z'|]$ is the attenuation kernel, also depending on the source angular distribution chosen where $\mu_m(E_\gamma)$ is the gamma ray mass absorption coefficient.

Much of the wide disagreement among various bremsstrahlung calculations can be traced to assumptions made about either the incident electron angular distribution expected in the problem or the angular distribution of the bremsstrahlung source. Perhaps the least conservative assumption about the source distribution that can logically be made for deep penetrations is that it is isotropic, and the most conservative assumption is that all the photons are emitted normally into the slab. In the first case the attenuation kernel is given by:

$$
G[\mu_m(E_\gamma)|Z-Z'|] = \frac{E_1[\mu_m(E_\gamma)|Z-Z'|]}{2} \quad , \qquad (48)
$$

where E_1 is the first exponential integral and plane isotropic buildup factors are used[8]. In the second case the attenuation kernel is

$$
G[\mu_m(E_\gamma)|Z-Z'|] = e^{-\mu_m(E_\gamma)|Z-Z'|} \quad , \qquad (49)
$$

and plane monodirectional buildup factors are used. Goldstein[7] tabulates these for infinite media, which should give a conservative estimate of the dose. These should be used cautiously, however, because they do not extend low enough in energy and extrapolation is dangerous. Figure 20 gives a comparison of these two cases for a half-space isotropic electron spectrum of exponential form incident on an aluminum shield with a water receiver (simulating tissue). Plane isotropic buildup factors were used in both calculations so that the difference observed is caused by the attenuation kernel. Actually, if correct buildup factors were used, the normal incident source case would be slightly lower.

Because of the built-in bias of using the extrapolated range in the straight-ahead approximation for calculating the source distribution, it is felt that there is no need to use the most conservative source angular distribution. Instead it is assumed that the bremsstrahlung source is half-space isotropic toward the receiver by the attenuation function given in Equation (48) multiplied by a factor of two. Still, the plane isotropic buildup factors[8] are used, making the calculation slightly more conservative. Figure 20 shows the results of an MSFC bremsstrahlung calculation for a half-space isotropic electron spectrum of exponential form incident on an aluminum shield with a water receiver (simulating tissue). Comparing Figs. 19 and 20 reveals that the MSFC calculation

(Fig. 20) is the most conservative of the three up to 4 or 5 g/cm^2. Above that depth, the monodirectional source calculation is more conservative by as much as a factor of three compared to the MSFC results.
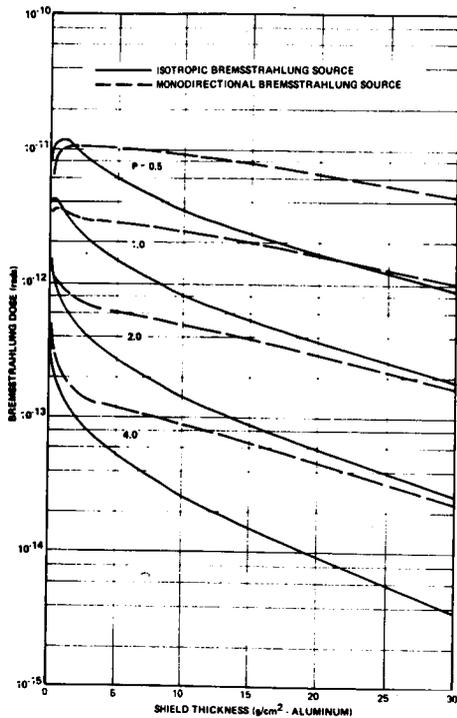

FIGURE 19: COMPARISON OF BREMSSTRAHLUNG DOSE CALCULATED ASSUMING AN ISOTROPIC SOURCE AND A MONODIRECTIONAL SOURCE DIRECTED NORMALLY INWARD FOR A HALF-SPACE ISOTROPIC INCIDENT ELECTRON SPECTRUM OF THE FORM $\Phi_0(E) = P \exp(-PE)$ e/cm^2 - MeV
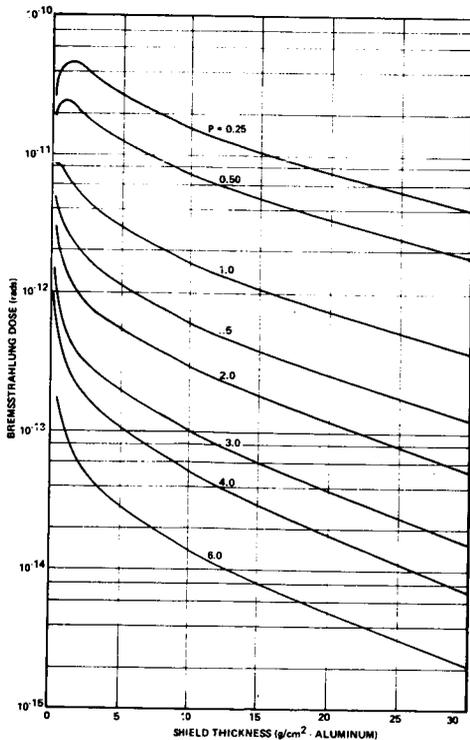

FIGURE 20: BREMSSTRAHLUNG DOSE CALCULATIONS ASSUMING A HALF-SPACE ISOTROPIC SOURCE FOR A HALF-SPACE ISOTROPIC INCIDENT ELECTRON SPECTRUM OF THE FORM $\Phi_0(E) = P \exp(-PE)$ e/cm^2 - MeV

Since the bremsstrahlung dose calculational method described so far involved triple or quadruple numerical integration and since the functions integrated are exceptionally difficult to integrate, the calculation can be performed conveniently only on a relatively large computer. In many cases, all that is needed is a rough order of magnitude estimate useful only in determining if a problem exists. For space applications, where most of the electron spectra encountered fall off exponentially with increasing energy, a conservative estimate of bremsstrahlung dose can be calculated as follows:

First, assume that all the electrons penetrate to the source plane and that at that plane their energy is the average energy of an external electron. That is,

$$\overline{E} = \frac{\int_{\overrightarrow{\Omega}} \int_{E'} E' \Phi_0(E',\overrightarrow{\Omega}) \, dE' \, d\overrightarrow{\Omega}}{\int_{\overrightarrow{\Omega}} \int_{E'} \Phi_0(E',\overrightarrow{\Omega}) \, dE' \, d\overrightarrow{\Omega}} \quad . \quad (50)$$

According to Evans[9], the total source in MeV/g is approximated by

$$S = H \, Z_0 \, \overline{E}^2 \int_{\overrightarrow{\Omega}} \int_{E'} \Phi_0(E',\overrightarrow{\Omega}) \, dE' \, d\overrightarrow{\Omega} \quad , \quad (51)$$

where H is a constant and Z_0 is the shield material atomic number. Berger and Seltzer[3] tabulate H for a cosine law electron source as a function of incident electron energy and shield thickness. Because the variation in the table is not great, a typical value 4×10^{-4} can be used for this approximation.

Second, assume that the source plane is located at half the extrapolated range at $\overline{E}$. The bremsstrahlung dose is given by:

$$D(Z) = K \, \mu_E \, S \, B[\overline{E}, \mu_m(\overline{E}) Z^*] E_1[\mu_m(\overline{E}) Z^*] \, . \, (52)$$

For μ_E, the energy absorption coefficient in the receiver, 0.033 cm^2/g is used, which is an upper bound on the coefficient for water in the range above 0.1 MeV. The source-receiver distance is given by:

$$Z^* = Z - R(\overline{E})/2 \qquad Z > R(\overline{E})/2 \quad . \quad (53)$$

A rough fit of the buildup factor in aluminum is given by: $B(\overline{E}, \mu_m(\overline{E}) Z^*) =$

$$1.0 + 26.47 \, \mu_m(\overline{E}) \, Z^* \overline{E}^{1.161} \qquad \overline{E} < 0.1 \qquad (54)$$

$$1.0 + 1.827 \, \mu_m(\overline{E}) \, Z^* \qquad 0.1 \leq \overline{E} \leq 0.2016$$

$$1.0 + 1.253 \, \mu_m(\overline{E}) \, Z^* \overline{E}^{-0.2354} \qquad 0.2016 < \overline{E} \leq 2.0$$

$$1.0 + 1.528 \, \mu_m(\overline{E}) \, Z^* \overline{E}^{-0.522} \qquad \overline{E} > 2.0 \quad .$$

Simplifying somewhat for an aluminum shield and a water receiver yields

$$D(Z) = 2.7 \times 10^{-12} \overline{E}^2 B[E, \mu_m(\overline{E}) Z^*]$$

$$E_1[\mu_m(\overline{E}) Z^*] \int_{\overline{\Omega}} \int_{E'} \Phi_0(E', \overrightarrow{\Omega}) dE' d\overrightarrow{\Omega} \qquad (55)$$

Figure 21 shows the result of a bremsstrahlung dose calculation using Equation (55); Fig. 22 shows a similar calculation assuming a monodirectional source. As can be seen in comparisons with results of more accurate calculations, the approximation yields reasonable order of magnitude estimates that are generally conservative.
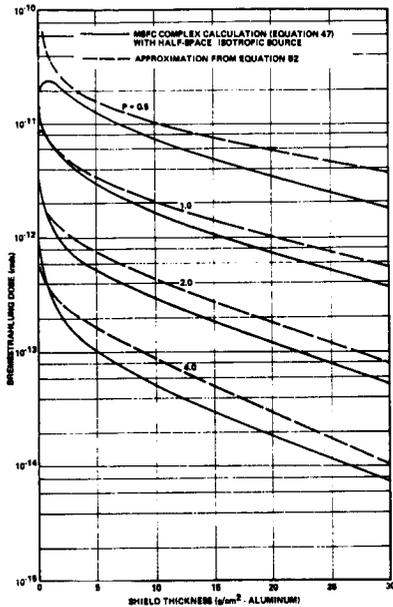

FIGURE 21: COMPARISON OF BREMSSTRAHLUNG DOSES CALCULATED ASSUMING A HALF-SPACE ISOTROPIC SOURCE AND INCIDENT SPECTRUM IN THE COMPLEX MSFC CALCULATION [EQUATION (47)] AND USING EQUATION (52). THE SPECTRUM IS OF THE FORM $\Phi_0(E) = P \exp(-PE)$ e/cm² - MeV
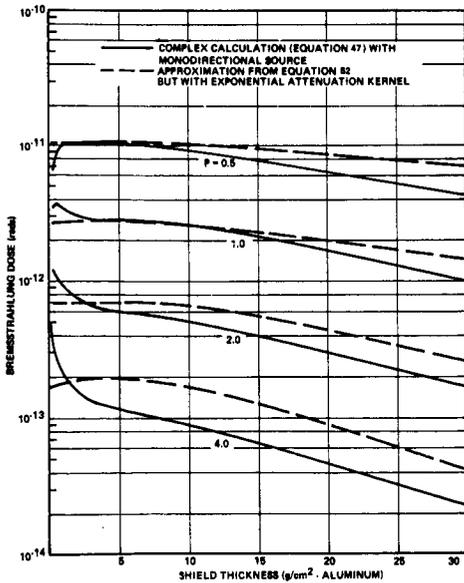

FIGURE 22: COMPARISON OF BREMSSTRAHLUNG DOSE CALCULATED ASSUMING A MONODIRECTIONAL SOURCE DIRECTED NORMALLY INWARD AND A HALF-SPACE ISOTROPIC ELECTRON SPECTRUM OF THE FORM $\Phi_0(E) = P \exp(-PE)$ e/cm² - MeV IN THE COMPLEX MSFC CALCULATION [EQUATION (47)] AND USING EQUATION (52) BUT WITH AN EXPONENTIAL ATTENUATION KERNEL

CONCLUSION

Although the results of the different electron and bremsstrahlung dose calculations developed at MSFC give results in relatively good agreement with each other, comparison with independent calculation is useful in pointing up areas of possible weakness. Wayne Scott of Oak Ridge National Laboratory has made such calculation using a Boeing program called Charge and a Douglas program called BEP as well as an older version of the MSFC program using Berger's transmission and reflection data[10]. The spectrum used was

$$\Phi_0(E) = 3.88 \, e^{-0.575E - 0.055E^2} \frac{e}{cm^2 - MeV - sec}, \quad (56)$$

which was renormalized to a total flux of unity. Table 3 gives the calculated electron dose in units of rad/h behind an aluminum shield on a tissue receiver for a normally incident beam. The MSFC results shown are for the new program using Berger's energy deposition coefficients and for the straight-ahead approximation. Both the MSFC program results are higher than the Charge and BEP results. The calculation using Berger's data is believed to be higher because the receiver had infinite backing behind it, whereas the other programs assume no backing. The straight-ahead calculation was higher because the extrapolated range was used in describing the transport.

Scott also did some spectral calculation at 0.5 and 1.0 g/cm² for the same incident spectrum using Charge, BEP, and Berger's Monte Carlo program, ETRAN. Figures 23 and 24 show these results plus spectra calculated with the MSFC straight-ahead program; it can be seen why the straight-ahead program yields higher doses. For the low-energy end of the spectrum consisting of particles that have lost the largest fraction of their energy and have been scattered the most, the straight-ahead program overestimates the flux by as much as a factor of three compared to ETRAN. For higher energies there is relatively good agreement with ETRAN. The overestimate of the low-energy component of the electron flux will be reflected in the bremsstrahlung calculation as an overestimate of the low-energy component of the bremsstrahlung source and in turn an overestimate of the bremsstrahlung dose, especially behind the thin shield where the low-energy bremsstrahlung has not been attenuated greatly.
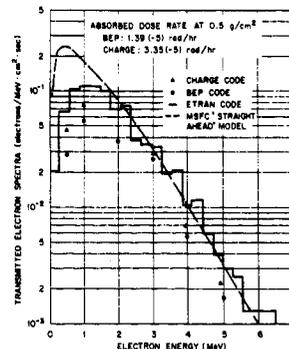

Figure 23. Transmitted electron spectra behind a semi-infinite slab of aluminum of thickness 0.5 g/cm².

In conclusion, the program using Berger's energy deposition data should be preferred for dose calculations, because in most practical problems the receiver does have effectively infinite backing and because the program is relatively easy to use. Where an electron spectrum at an internal point in a shield is needed, the straight-ahead approximation can be used to obtain a conservative estimate of the differential flux. For first-order calculations an estimate of bremsstrahlung dose can be obtained by using Equation (55) where the incident electron spectrum falls off exponentially. Where an accurate calculation is needed, Equation (47) with a half-space isotropic attenuation kernel should be used. More work needs to be done here in determining the actual source angular distribution.
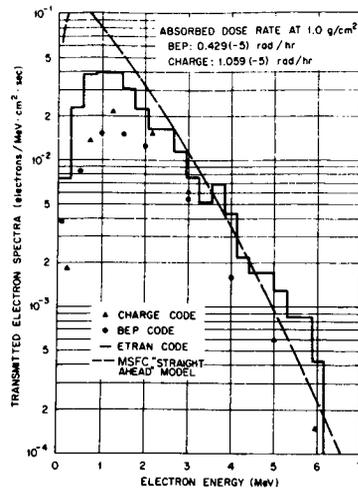

Figure 24. Transmitted electron spectra behind a semi-infinite slab of aluminum of thickness 1.0 g/cm².

REFERENCES

1. BERGER, M.J.: Diffusion of Fast Charged Particle. Methods in Computational Physics, vol. 1, Academic Press, 1963, p. 135.

2. BERGER and SELTZER: Tables of Energy Losses and Ranges of Electrons and Positrons. NASA SP-3012, 1964.

3. BERGER and SELTZER: Penetration of Electrons and Associated Bremsstrahlung Through Aluminum Targets. Protection Against Space Radiation, NASA SP-169, 1968.

4. RESTER, D.H.; DANCE, W.E.; and DERRICKSON, J.H.: Thick Target Bremsstrahlung Produced by Electron Bombardment of Targets of Be, Sn, and Au in the Energy Range 0.2 - 2.8 MeV. J. Appl. Phys., vol. 41, no. 6, May 1970, p. 2682.

5. FLAMMERSFELD, A.: Naturw, vol. 33, 1946, p. 280.

6. KOCH, H.W.; and MOTZ, J.W.: Bremsstrahlung Cross-Section Formulas and Related Data. Rev. Mod. Phys., vol. 31, no. 4, October 1959, p. 920.

7. GOLDSTEIN, H.: Fundamental Aspects of Reactor Shielding. Addison-Wesley Publishing Company, 1959, p. 237.

8. BURRELL, M.O.; and WATTS, J.W.: Plane Isotropic Buildup Factors for Bremsstrahlung Calculations. NASA-TND-4096, August 1967.

9. EVANS, R.: The Atomic Nucleus. McGraw-Hill Book Company, Inc., 1955, p. 617.

10. SCOTT, W.W.: Comparison of the Results Obtained with Several Electron-Penetration Codes. ORNL RSIC-28.